OBSERVATIONAL STUDIES RELEVANT FOR THE VERIFICATION OF THE GENERAL CIRCULATION MODELS

E.O. Holopainen
Department of Meteorology
University of Helsinki

Abstract

Uncertainties in our knowledge concerning the observed climate are first reviewed in light of recent intercomparisons of two large northern hemisphere data sets, which should both represent the same conditions. These uncertainties appear large in data-sparse oceanic areas and have to be taken into account when intercomparison of different models is performed.

Recent observational results on the effect of large-scale transient eddies on the time-mean flow are then reviewed and some new results presented which could be of value for model verification. By means of a diagnosis of relevant terms in the budgets of potential enstrophy and energy it is shown that in both winter and summer the transient eddies exert a strong dissipative effect on the stationary disturbances in the troposphere. This dissipaiton is caused primarily by long-period (10-90 d) fluctuations, which appear to be effective smoothers of the longitudinal differences in the time-mean temperature.

The effect of the time-mean flow on the transient eddies is discussed in terms of the energetics of these eddies. In addition to advective effects the mean flow appears to affect the eddy energy particularly through the "baroclinic conversion" mechanism, which is important in the northern hemisphere winter especially near the western coasts of the two oceans. Only semi-quantitative estimates can be given at the present time for the geographical distribution of many of the terms in the energy budget of the transient eddies.

At the end of the paper some recommendations are made on the observational work that needs to be done in future.

1. INTRODUCTION

When the behaviour of a general circulation model (GCM) is to be compared with that of the real atmosphere, one normally integrates the GCM for a sufficiently long time so that a statistically stationary state is reached, and compares the statistics of the model with those obtained from observations of the real atmosphere.

Some of the recent observational studies relevant for this purpose are listed in Table I. From the studies concerning the basic variables (Group A) one could mention the "NMC atlas" prepared by Lau et al. (1981) and the "GFDL atlas" by Oort (1982), which describe the "observed" climate of the free atmosphere on the basis of two independently analyzed long-term data sets. In addition to the fields of time-mean quantities these atlases also contain fields of some important variances and covariances. As an example, Fig. 1 shows the standard deviation of temperature at 850 mb and variance of the meridional wind component for the northern extratropics in winter. This figure illustrates one aspect which has not come out from the earlier well-known data compilations (e.g. Oort and Rasmusson, 1971). It is the large longitudinal variation: temperature variance (transient eddy available potential energy) has maxima over the continents, wind variance (transient eddy kinetic energy) over the oceans. These are important features to be simulated in a GCM.

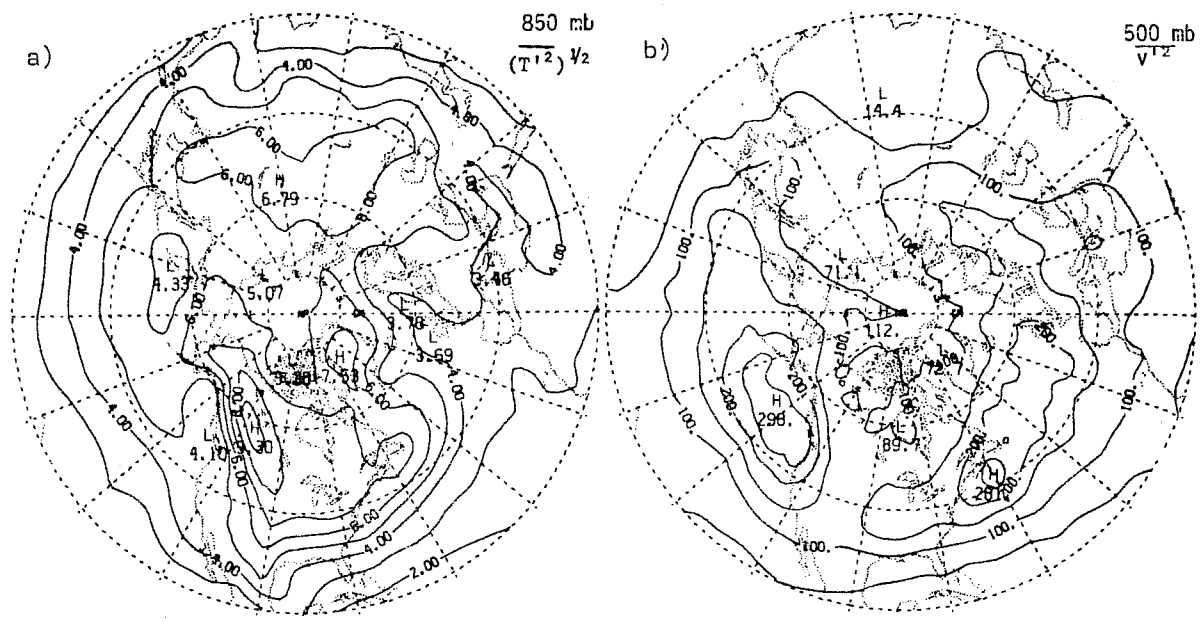

Fig. 1 Wintertime distribution of
a) standard deviation of temperature, $(\overline{T'^2})^{1/2}$, at 850 mb (in K),
b) variance of the meridional wind component, $\overline{v'v'}$, at 500 mb (in $m^2 s^{-2}$)
according to NMC data (from Lau et al., 1981, Figs. II B2 and II B4)

Table 1. Examples of observational studies relevant for the verification of the GCM's.

A.	STATISTICS ON BASIC ATMOSPHERIC VARIABLES
1.	Zonally-averaged statistics (Oort and Rasmusson, 1971; Newell et al., 1972/74)
2.	Geographical (λ,ϕ) patterns of the statistics (Blackmon, 1976; Lau et al., 1981; Oort, 1982; Trenberth, 1981; White, 1982)
3.	Interannual variability of circulation statistics (Madden, 1976; Oort, 1977; van Loon, 1978; Speth and Frenzen, 1982)
4.	FGGE data (Bengtsson et al., 1981)
B.	INTERCOMPARISONS
1.	Intercomparison of different "observed" data sets (Arpe, 1980; Trenberth and Paolino, 1980; Lau and Oort, 1981/82)
2.	Intercomparison of "observed" and "calculated" climate (Blackmon and Lau, 1980)
3.	Intercomparison of different "calculated" data sets (JOC, 1979; Bengtsson and Lange, 1982)
C.	STUDIES ON BALANCE REQUIREMENTS
1.	Boundary conditions (at the lower and upper boundary) (Budyko, 1963; Hastenrath, 1980; Stephen et al., 1981)
2.	Energy, momentum, vorticity etc. (Newell et al., 1972/74; Peixoto and Oort, 1974; Lau, 1979a,b; Holopainen et al., 1982; Wei et al., 1982)
D.	STATISTICS ON PRECIPITATION AND CLOUDINESS
1.	Precipitation (UNESCO, 1974; Jaeger, 1976; Atlas and Thiele, 1982)
2.	Cloudiness (Berlyand and Strokina, 1980; Schiffer, 1982)

Going back to Table 1, intercomparisons (Group B) have provided preliminary information on the confidence limits for the "observed" climate and on the performance of some GCM's. New data from satellites and results from several diagnostic analyses have elucidated the way in which different physical balance requirements are fulfilled in the climate system (Group C). Precipitation and cloudiness (Group D in Table 1) are examples of high-priority climate variables which are not well known. Measurement of precipitation from satellites may be possible in future (Atlas and Thiele, 1982). For cloudiness, the International Satellite Cloud Climatology Project (ISCCP) of WMO/ICSU Join Scientific Committee (Schiffer, 1982) is likely to provide data which will probably be important for the verification and further development of GCM's.

In the following, uncertainties in the "observed" climate are first discussed in section 2 by reviewing results of some recent studies. In section 3 new results of potential importance for model verification are presented on the interplay between the time-mean flow and the transient eddies. In particular, some recent findings on the maintenance of stationary (time-mean) eddies, which appear to be a problem in many GCM's, are emphasized and the geographical variation in the energetics of the transient eddies is discussed. In section 4 some suggestions for further work are made.

2. CONFIDENCE LIMITS OF THE "OBSERVED" CLIMATE

With what accuracy do we know the climate variables in different parts of the atmosphere? Fig. 2 shows the difference in the 9-winter mean temperature at 850 mb between two data sets, which are both based essentially on the same radiosonde observations but have different data analysis procedures (Lau and Oort, 1981). The temperature differences over the data-rich areas of North America and Europe appear to be rather small. Over the data-sparse areas of the North Pacific, however, large areas are found where the magnitude of the temperature difference is larger than 2K both in winter and summer. At 30^{o}N the zonally-averaged value of this difference in winter is 1 K. Lau & Oort are unable to infer which one of the two data sets is in general the more correct. Large differences between the climatological upper-level grid-point analyses (based upon the same radiosonde data) have been reported also by Arpe (1980) and Parker (1980). Thus the absolute values of time-mean temperature (and of other climate variables) have a relatively large margin of error in the Northern Hemisphere and much more in the Southern Hemisphere (see also Oort, 1978).

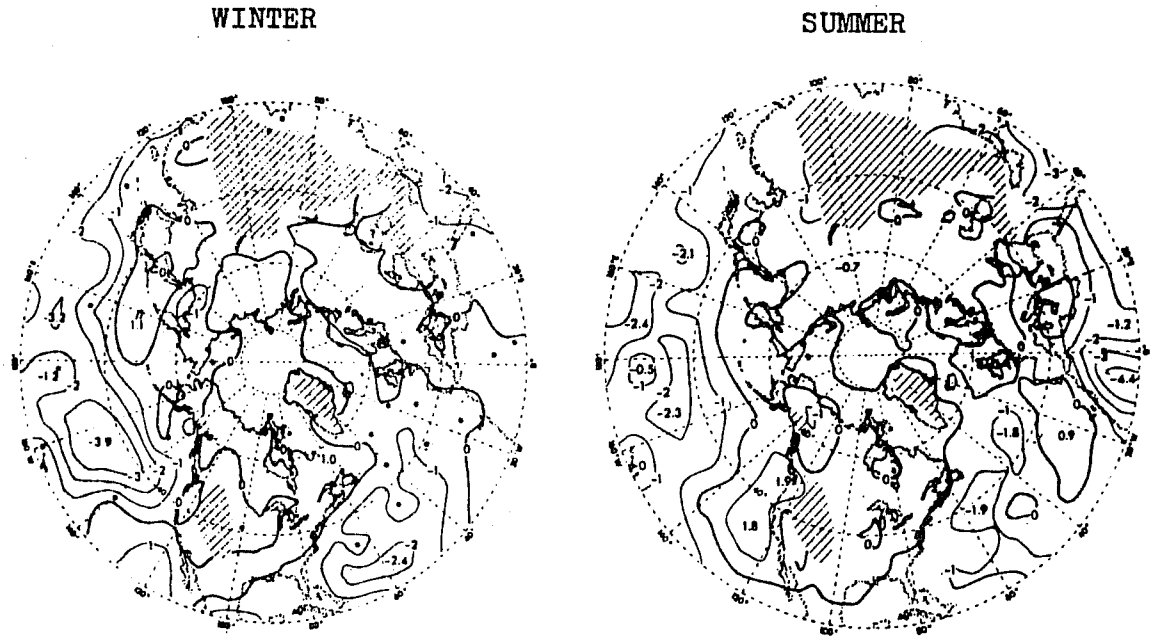

Fig. 2 Distribution of the 9-year average 850 mb temperature difference between the GFDL analysis and the NMC analysis (GFDL - NMC) in winter (left) and in summer (right). (From Lau and Oort, 1981, Figs. 10c and 12d).

Fig. 3 Vorticity advection over the North Pacific region in different latitudes in December-February according to the GFDL data (dashed-dotted curve) and the NMC data (dashed curve). The values are longitudinal averages over the ocean basin. For comparison, the continuous line shows the values of the surface stress curl determined from surface data. All the curves should in principle coincide. (From Holopainen and Oort, 1981b).

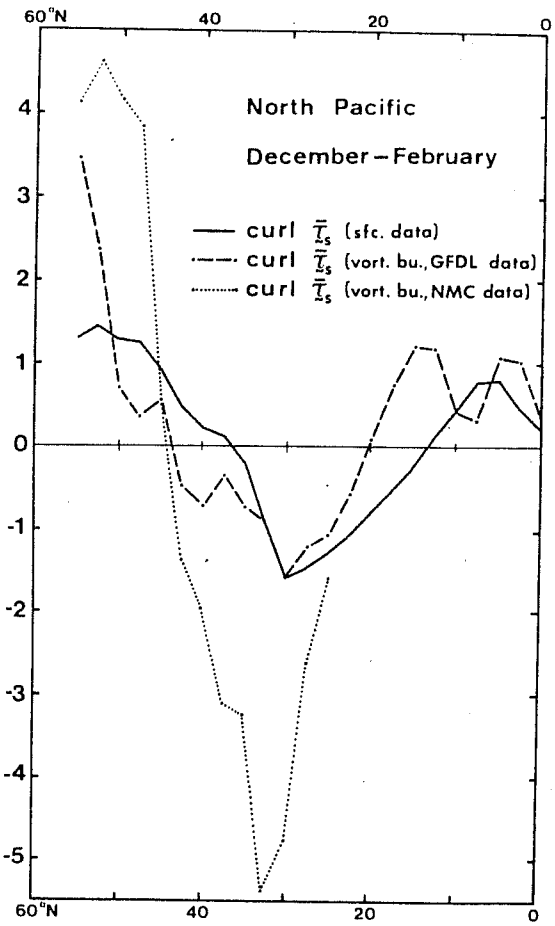

The warning from Fig. 2 is twofold. First, the uncertainty in the "observed" conditions can be very large in data-sparse regions and must be taken into account when a GCM is compared with reality or with another GCM. Second, the present grid-point data must not be used for the determination of climate trends, because large spurious trends most probably exist in such data owing to intermittent changes in the analysis system (see also Parker, 1980).

If uncertainty is large for such basic quantities as mean temperature, it can be expected to be much larger for more delicate, higher-order climate variables. Fig. 3 shows the vertically-intergrated time-mean vorticity advection over the North Pacific calculated from the "GFDL data" and the "NMC data" (Holopainen and Oort, 1981b). The difference between the estimates obtained from the two data sets is huge. In this particular case, the estimate from the GFDL data agrees better with an independent estimate based upon surface winds than that from the NMC data. This should not, however, be interpreted to imply that the GFDL data are in general better than the NMC data.

3. ON THE BALANCE REQUIREMENTS OF THE TIME-MEAN FLOW AND THE TRANSIENT EDDIES

Formally, an arbitrary quantity $s = s(\lambda, \phi, p, t)$ can be written as

$$s(\lambda, \phi, p, t) = \bar{s}(\lambda, \phi, p, \Delta t_s) + s'(\lambda, \phi, p, t, \Delta t_s)$$

where $\bar{s}$ is the time-mean (over sampling duration Δt_s) and s' the transient part of s ($\overline{s'} = 0$). Following a common terminology, all quantities containing s' will be referred to below as transient eddy (TE) quantities.

A natural first step in the verification of a GCM is a direct comparison of "calculated" and "observed" fields of time-means, $\bar{s}$, and variances, $\overline{s'^2}$, of certain key variables. In the second stage one may wish to make an analysis of the way in which different physical balance requirements are fulfilled in the model as compared with the real atmosphere, i.e. one wants to make budget studies. In recent years several diagnostic studies (e.g. Lau, 1979a,b; Holopainen and Oort, 1981b) have revealed important geographical variations in the "observed" time-mean budgets of heat, vorticity etc.. Such variations should, of course, also be simulated by a good GCM.

In the following we consider primarily one specific aspect of such budget studies, namely the interplay between the time-mean flow and the transient eddies. However, many other aspects will also be touched upon.

The results to be presented are based on two observational grid-point data sets: an 8-year NMC data set for the wintertime northern extratropics and a 5-year global "GFDL data" set for December-February and June-August. The data used here are the same as in Holopainen et al. (1982) and are a subset of the larger data sets described in Lau and Oort (1981). With these data the time-mean thus refers to an ensemble-mean over several winters (or summers) and the transient eddies also contain, in addition to the synoptic fluctuations within a season, a (small) part arising from the interannual fluctuations.

3.2 The effect of TE on the time-mean flow

The transient eddies transport heat, momentum etc. and in doing so they exert a forcing effect on the time-mean flow. One way of looking into this effect is to consider the budget of the time-mean potential vorticity, which can be written symbolically as (e.g. Holopainen et al., 1982):

$$\frac{\partial \bar{q}}{\partial t} = \left(\begin{matrix}\text{Horizontal}\\ \text{adv. term}\end{matrix}\right) + \left(\begin{matrix}\text{Heating}\\ \text{term}\end{matrix}\right) + \left(\frac{\partial \bar{q}}{\partial t}\right)_T + \ldots = 0 \qquad (1)$$

where

$$\bar{q} = \bar{\zeta} + f - f \frac{\partial}{\partial p}\left(\frac{\bar{\theta}''}{\tilde{S}}\right) \qquad (2)$$

is one form of time-mean potential vorticity, ζ relative vorticity, f Coriolis parameter and $S = -\frac{\partial \theta}{\partial p}$ the static stability. The symbol $\tilde{(\ )}$ denotes an area average on a pressure surface and $(\ )''$ a deviation from it. Otherwise the notation is conventional.

The term $\left(\frac{\partial \bar{q}}{\partial t}\right)_T$ in (1) represents the local tendency of $\bar{q}$ due to horizontal TE fluxes of heat and vorticity:

$$\left(\frac{\partial q}{\partial t}\right)_T = D = D^{HEAT} + D^{VORT} \qquad (3)$$

where

$$\begin{cases} D^{HEAT} = f \frac{\partial}{\partial p}\left(\frac{\overline{\nabla \cdot \theta' \mathbf{v}'}}{\tilde{S}}\right) & (4) \\ D^{VORT} = -\nabla \cdot \overline{\zeta' \mathbf{v}'} \,. & (5) \end{cases}$$

A convenient aspect of the potential vorticity equation is thus that it combines the heat transfer properties and the momentum transfer properties of the transient eddies into a single dynamic framework in which they can be compared with each other. A complication with this equation is that if it has to be solved for the stream function (or geopotential) tendencies caused by the transients, TE effects arise not only from the terms D^{HEAT} and D^{VORT} but also, via the boundary conditions, from the TE heat fluxes at the lower and upper boundary. Here, however, we will be dealing only with the effect of transient eddies in the budget of potential enstrophy; for such budget studies only the "interior" TE forcing term D is needed.

One way of picturing the field of D ($\hat{=} -\nabla.\overline{q'\mathbf{v}'}$) is to show patterns of χ_q, defined by

$$\nabla^2\chi_q = D$$

The irrotational part of the potential vorticity flux, $(\overline{q'\mathbf{v}'})_\chi$, is then given by

$$(\overline{q'\mathbf{v}'})_\chi = -\nabla\chi_q$$

Isolines of χ_q can also be interpreted as isolines of stream function for a nondivergent horizontal force $(\overline{q'\mathbf{v}'})_\chi \times \mathbf{k}$, the curl of which is D (Holopainen et al., 1982).

Fig. 4 shows the pattern of χ_q in the 300-700 mb layer for the northern hemisphere winter and summer. Because $\bar{q}$ has a maximum at the north pole, the figure implies a down-gradient (southward) TE flux of potential vorticity and an essentially westward-directed "force" acting on the time-mean flow, stronger in winter than in summer. (The zonally-averaged value of this force is equal to the divergence of Eliassen-Palm flux (see Edmon et al. (1980)). The maps of "observed" and "calculated" χ_q can possibly be used as one means in the verification of a model's ability to simulate the TE forcing.

A physical interpretation of the results in Fig. 4 is that the TE horizontal heat fluxes, which in this context appear to dominate over the TE momentum fluxes, tend to smooth out the mean meridional temperature gradient and hence the baroclinic component of time-mean flow (Holopainen et al., 1982). Further interpretation in terms of energetics is given in section 3.3.

Some "observed" results are shown in the following for the TE forcing of stationary eddies, which imply important longitudinal variations in the Earth's climate and are perhaps less understood than the zonally-averaged axisymmetric climate. They appear to be a problem in many GCM's.

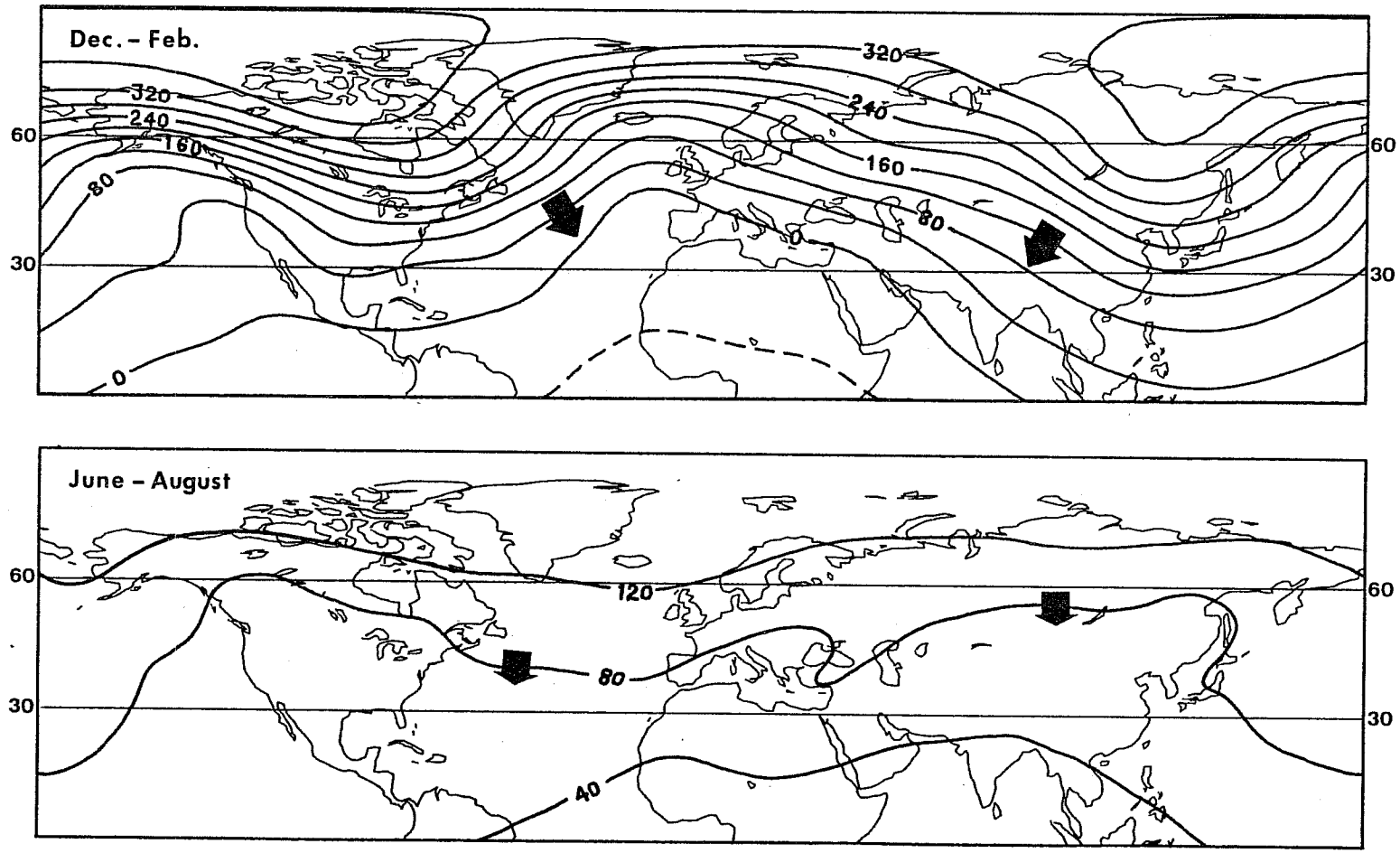

Fig. 4 Isolines of χ_q illustrating the "interior" TE effect on the time-mean flow in the 300 - 700 mb layer in winter (upper panel) and in summer (lower panel). The pattern is obtained by solving the Poisson equation $\nabla^2\chi_q = D$, when D has the expression (3) and is estimated from observations. The χ_q field determines the irrotational part of the TE flux of potential vorticity, $(\overline{q'\mathbf{V}'})_\chi = -\nabla\chi_q$, the direction of which is in the figure indicated by bold arrows. Spacing of isolines is 40 $m^2 s^{-2}$.

One measure of the intensity of the stationary eddies is their **potential enstrophy**

$$B = 1/2 \quad [\bar{q}^{*\,2}] \qquad (6)$$

Here the bracket denotes zonal average and the asterisk deviation from this average. As can be seen from Eqs. (1) and (3), the TE transports enter the potential enstrophy budget of the stationary waves through the covariance quantity $(\frac{\partial B}{\partial t})_T = [D^* \bar{q}^*]$.

In Fig. 5 is shown the latitude-heigtht distributions of B and $(\frac{\partial B}{\partial t})_T$ for Northern Hemisphere winter, as computed with the GFDL and NMC data sets. The two data sets are seen to yield roughly the same results. The pattern for B is characterized by a primary maximum in the upper troposphere. The numerical values of potential enstrophy are an order of magnitude larger than those of enstrophy $1/2\ [\bar{\zeta}^{*2}]$ reported by Holopainen and Oort (1981b). It is hence evident that by far the most significant contribution to B comes from the term $-f \frac{\partial}{\partial p} (\frac{\bar{\theta}''}{\bar{S}})$ (see (2)).

The quantity $[D^* \bar{q}^*]$ is negative almost everywhere (Fig. 5, bottom panel). This is largely a reflection of the negative spatial correlation between D^{HEAT} and $\bar{q}$. Since we have concluded in the preceding paragraph that the largest contribution to $\bar{q}$ comes from the term $-f \frac{\partial}{\partial p} (\frac{\bar{\theta}''}{\bar{S}})$, the role of the transient eddies in the balance of B is seen to be essentially determined by the local influences of the eddy heat transports on the time-averaged static stability. In the present context, the effects of D^{VORT} on the enstrophy $1/2\ [\bar{\zeta}^{*2}]$, as examined by Holopainen and Oort (1981b), appear to play a less important role. The net damping effect of TE on the stationary eddies was first demonstrated by Youngblut and Sasamori (1980), who used data for January 1963.

Fig. 6 shows the distribution of B and $(\frac{\partial B}{\partial t})_T$, as calculated from the GFDL data, both for the northern winter and the northern summer. In summer the amount of enstrophy in the stationary eddies is seen to be smaller than in winter and more concentrated in the lower and upper troposphere. The effect of transient eddies is seen also dissipative (negative) in summer at most latitudes and pressure levels.

In order to get some idea of the time scale of the TE dissipation on the stationary eddies as a function of height we may calculate hemispheric averages of $(\frac{\partial B}{\partial t})_T$ and B at each pressure level. A measure of the TE effect is then the "frictional coefficient"

$$\nu^q = (-\widetilde{\frac{\partial B}{\partial t}})_T / \tilde{B} \qquad (7)$$

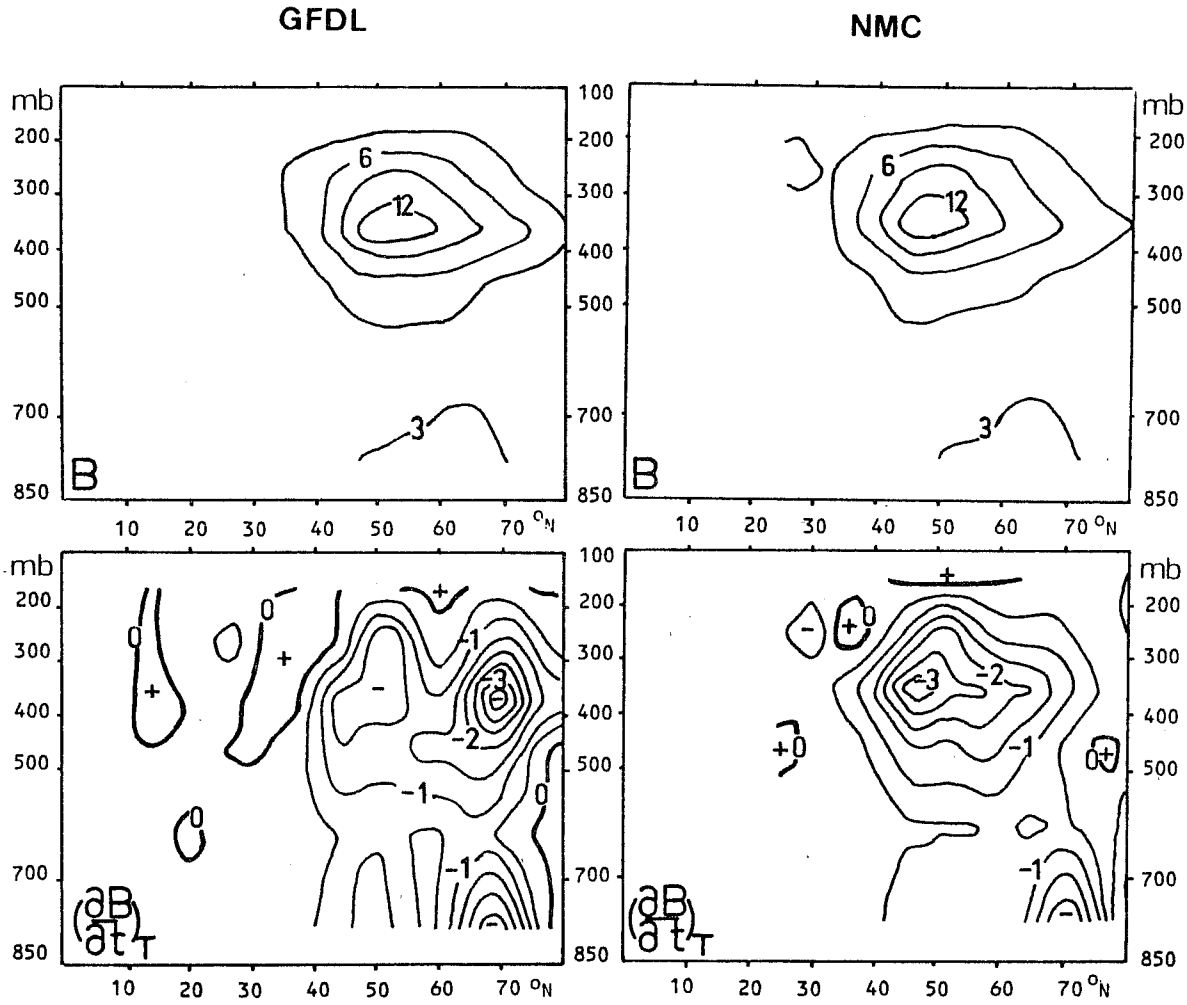

Fig. 5 Latitude-height distribution of $B = 1/2\,[\bar{q}^{*2}]$ *(in* $10^{-10}\ s^{-2}$*), and of* $\left(\frac{\partial B}{\partial t}\right)_T = [D^*\ \bar{q}^*]$ *(in* $10^{-15}\ s^{-3}$*) for winter as determined from GFDL data (left) and NMC data (right). (From Holopainen et al., 1982)*

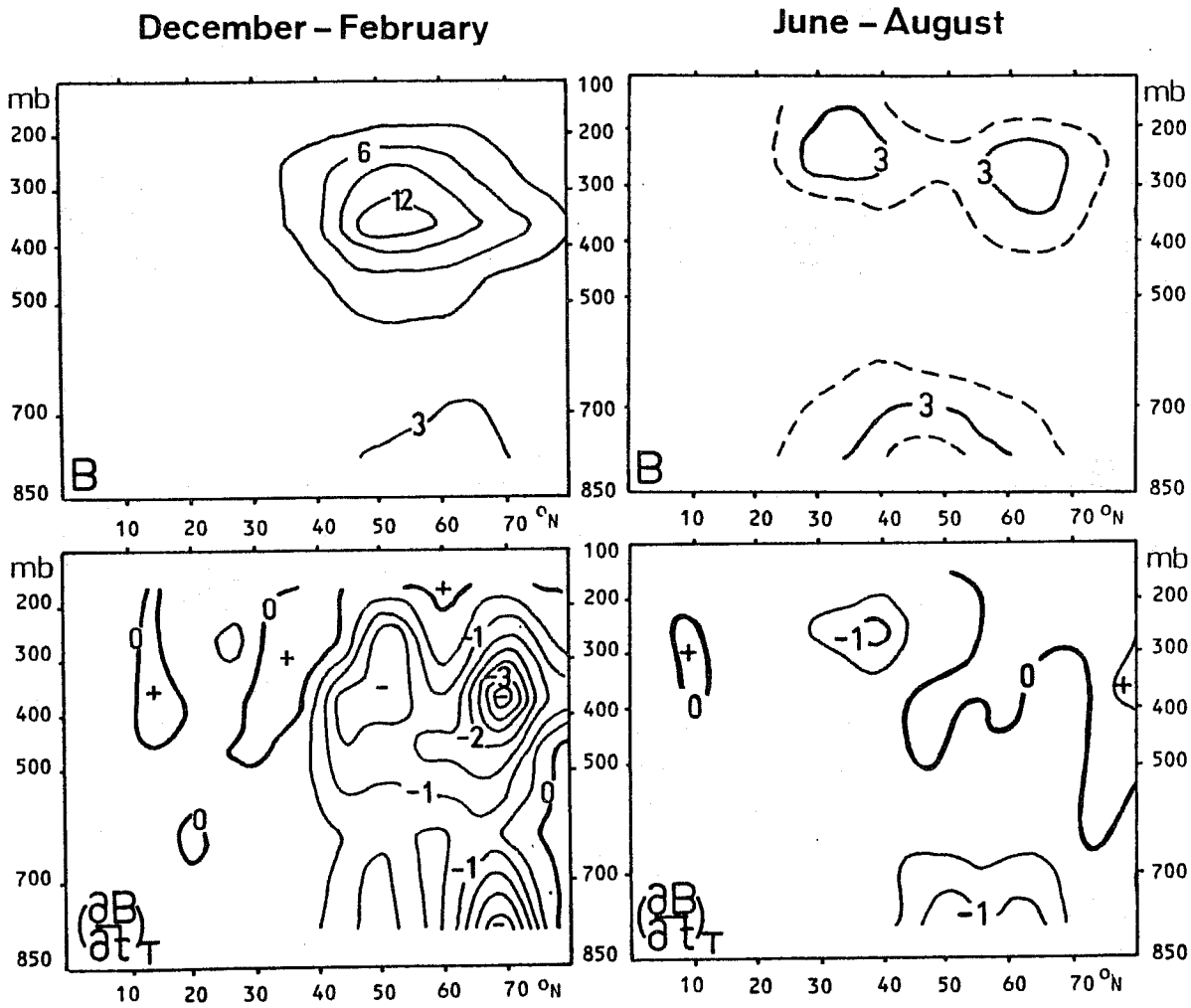

Fig. 6 Distribution of $B = 1/2\,[\bar{q}^{*2}]$ *and* $(\frac{\partial B}{\partial t})_T = [\bar{q}^* D^*]$ *over the Northern Hemisphere in December–February (left) and in June–August (right) estimated from the GFDL data. Units as in Fig. 5.*

where the circumflex denotes the hemispheric average. Note that $(\nu^q)^{-1}$ gives the e-folding time associated with the TE friction.

Fig. 7a shows ν^q as a function of pressure for both winter and summer. It is seen that the TE damping effect on the stationary eddies is larger in winter than in summer and much larger in the troposphere than in the lower stratosphere. The associated e-folding time is a few days in the troposphere and a few weeks in the lower stratosphere.

Because a major contribution to B comes from the third term in (2) and thus from the temperature field, results similar to those in Fig. 7a can also be expected from the budget of stationary eddy available potential energy. The results of Lau (1979b) concerning the TE effects on the mean temperature anomalies also support this. This idea is confirmed by Fig. 7b, which shows another "frictional coefficient" for the TE effects on the stationary eddies

$$\nu^a = (-\frac{\partial \widetilde{a_{SE}}}{\partial t})_T / \widetilde{a}_{SE} \cdot \qquad (8)$$

Here $$(\frac{\partial a_{SE}}{\partial t})_T = -1/2\, c_p \gamma \overline{T'V'} \cdot \nabla \overline{T}^*$$

is the rate of conversion of the available potential energy of the stationary eddies, denoted by a_{SE}, to that of the transient eddies (γ is a stability factor).

If the horizontal TE heat fluxes are such effective dampers of the stationary eddies, it is worth while having a closer look at them. Fig. 8 illustrates the irrotational part of the TE heat flux, from which the zonally-averaged part has been subtracted. (For the total irrotational TE heat flux, which is dominated by a strong poleward component, see Fig. 3 in Lau and Wallace, 1979). In winter the most significant features of this figure are (Fig. 8a) the flux divergence over the northeastern oceans and flux convergence over the northeastern continents, and the implied significant zonal heat fluxes. The corresponding heat fluxes in summer (Fig. 8b) are from the warm continents to the colder oceans. Thus, the TE heat fluxes exert both in winter and summer a damping effect on the longitudinal differences of the mean temperature.

Fig. 9 shows the contributions to the (total) horizontal heat flux divergence at 700mb in winter by long-period (10-90 d) and synoptic-period (2.5-6 d) fluctuations, according to the calculations by N-C. Lau. It is seen that the heat flux divergence in the northeastern oceanic areas arises from the long-period transients, which thus appear to be an effective damping mechanism for the stationary eddies.

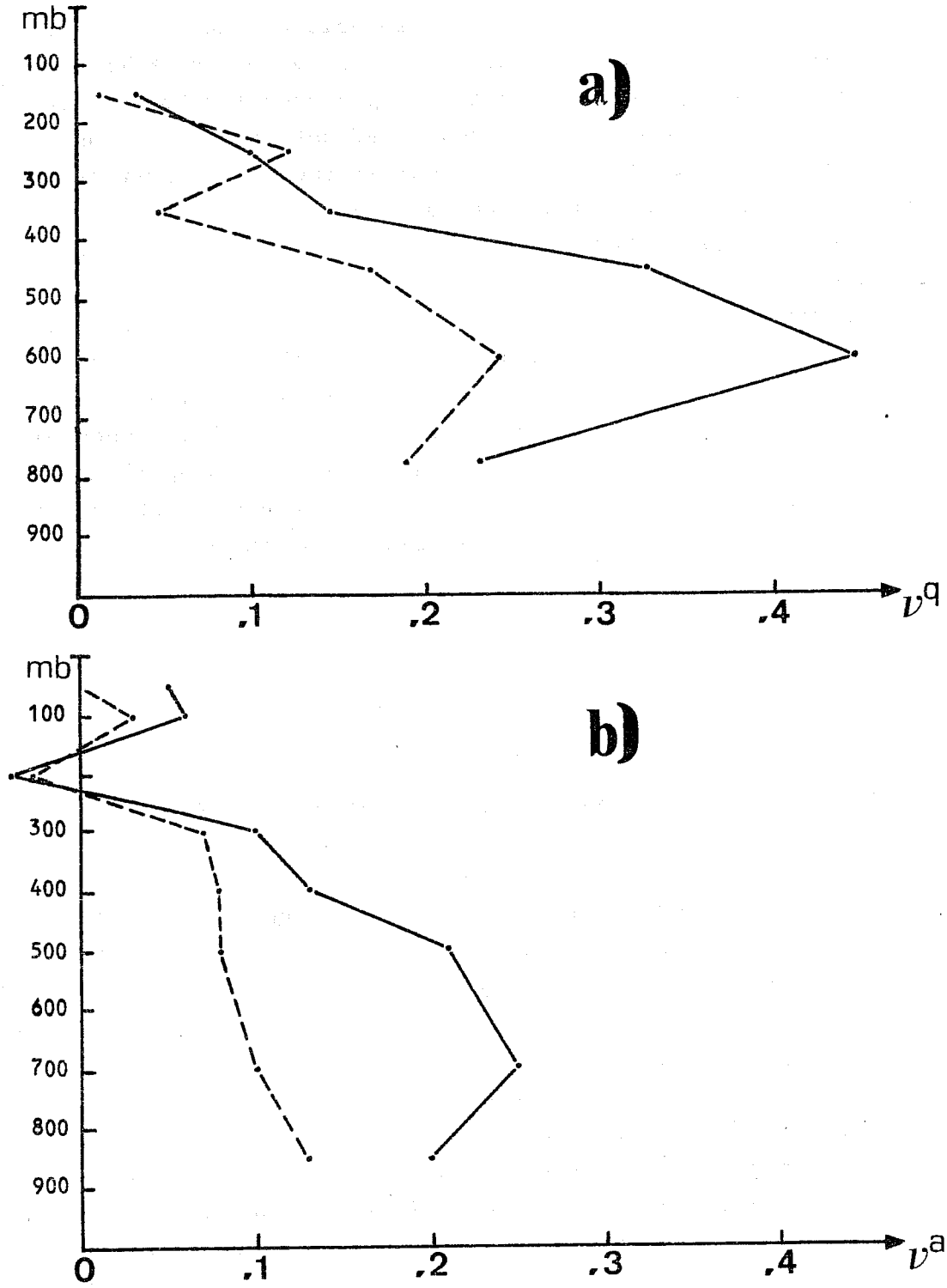

Fig. 7 a) The vertical profile of the damping coefficient ν^q as defined in (7) describing the dissipating effects of the transient eddies on the stationary eddies over the northern hemisphere. The solid (dashed) line is for December-February (June-August): Unit: 10^{-5} s^{-1}. (GFDL data).

b) As Fig. 7a but for the damping coefficient ν^a defined by Eq.(8).

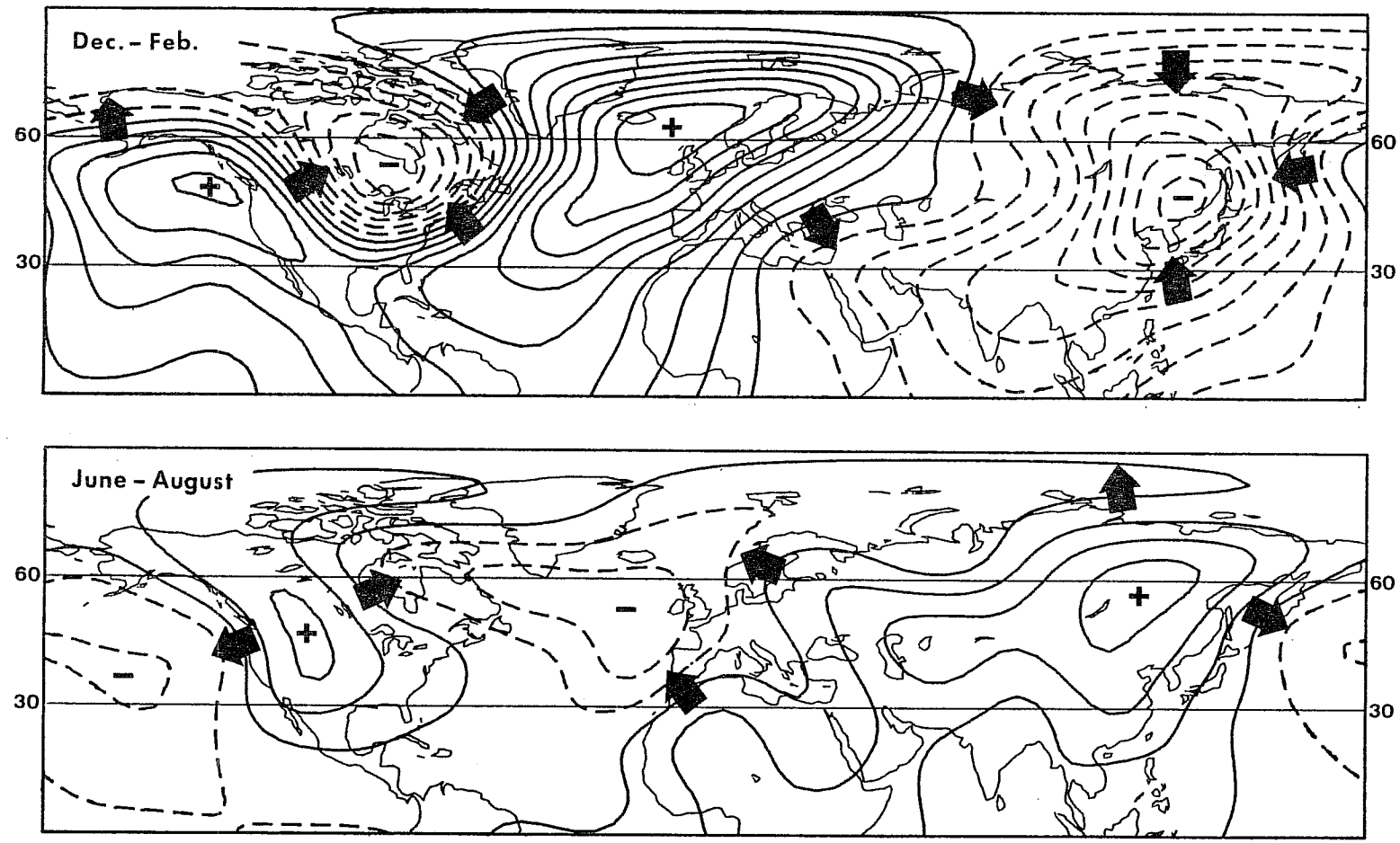

Fig. 8 The pattern of χ_h representing the irrotational heat flux $\boldsymbol{h} = (\overline{T'\boldsymbol{V}'} - [\overline{T'\boldsymbol{V}'}])_\chi$ such that $\nabla^2 \chi_h = \nabla \cdot \boldsymbol{h}$, at 850 mb in December-February (upper panel) and in June-August (lower panel). The vector $\boldsymbol{h}$ is perpendicular to the isolines of χ_h ($\boldsymbol{h} = \nabla \chi_h$) and its direction is indicated in the figure with some bold arrows. The centers of flux divergence (convergence) are indicated with a + (-) sign. Spacing of the isolines is 3×10^6 K m^2 s^{-1}.

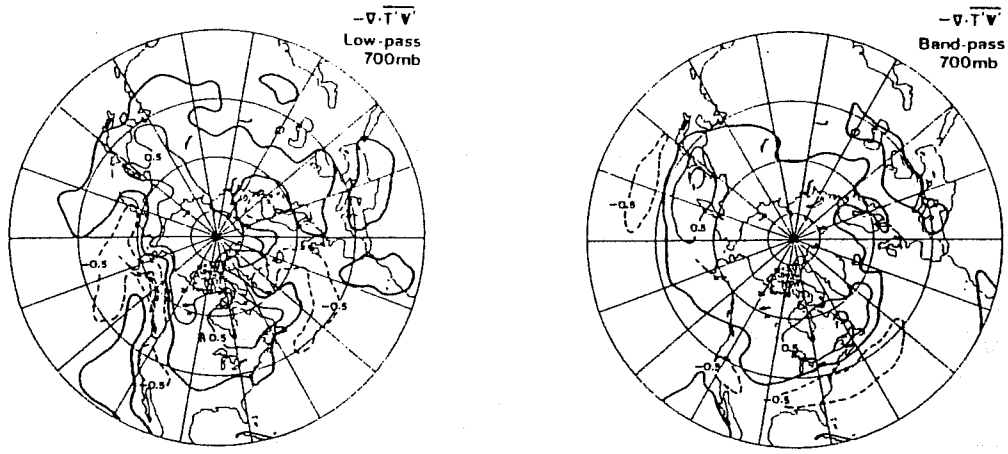

Fig. 9 Distribution of the convergence of the TE heat flux due to low-pass eddies (10-90 d; left panel) and the band-pass eddies (2.5-6 d; right panel) at 700 mb in winter. Unit: K d^{-1}. (Courtesy of N-C. Lau).

Although the effects of the TE momentum fluxes (vorticity fluxes) on the enstrophy and energy budgets of the stationary eddies are small in comparison with the TE heat fluxes, they are important in other ways. For example, they appear to be the major mechanism for compensating the loss of vorticity due to surface friction in the northern oceans (Holopainen and Oort, 1981b). Perhaps more importantly, they can cause pattern distortion and phase shift tendencies (such as the tendency to move the subtropical jet stream polewards) which do not enter the picture when enstrophy and energy budgets are discussed.

3.3 ON THE GEOGRAPHICAL VARIATION OF THE TRANSTENT EDDY ACTIVITY

As demonstrated by Fig. 1 the TE activity in the northern hemisphere has an aimportant longitudinal variation, the simulation of which with a GCM should be as important as the simulation of the time-mean flow.

One measure of the TE activity is the energy e_T defined as

$$e_T = a_T + k_T$$

where $a_T = 1/2\ c_p \gamma \overline{T'^2}$ is the TE available potential energy (γ is the stability factor) and $k_T = 1/2\ \overline{\mathbf{V}'^2}$ the TE kinetic energy per unit mass. Earlier diagnostic studies (e.g. Oort and Peixoto, 1976) show that in hemispheric averages over NH there is near equiparti-

tioning of e_T between a_T and k_T, and that in the lower troposphere a_T is larger than k_T whereas in the upper troposphere the reverse is true. Fig. 10 shows the geographical distribution of a_T, k_T and e_T at 500 mb, where the patterns are roughly the same as those for the vertically integrated quantities. It is seen that both a_T and k_T have maxima in the middle latitudes but have different longitudinal distribution: k_T has maxima over the oceans whereas the maxima of a_T are more connected with the continents. These are features which were already pointed out in connection with Fig. 1 for 850 mb.

In order to avoid the well-known difficulties in the estimation of the conversion between a_T and k_T we consider only the budget of e_T. The equation for the total amount of e_T in an air column at a location λ, ϕ can be written symbolically as

$$0 = Adv + (C_a + C_k + C_m) + (S_a + S_k) + (F_e + F_a + F_k) \qquad (9)$$

where the different terms have the following expressions:

$$Adv = -\int \nabla \cdot w e_T \bar{\mathbf{V}}\, dm \qquad (10)$$

$$C_a = -\int c_p \gamma \overline{T'\mathbf{V}'} \cdot \nabla \bar{T}\, w\, dm \qquad (11)$$

$$C_k = \int \{ -\frac{\overline{u'u'}}{a\cos\phi}\frac{\partial \bar{u}}{\partial \lambda} - \overline{u'v'}\cos\phi \frac{\partial}{a\partial\phi}\left(\frac{\bar{u}}{\cos\phi}\right) - \frac{\overline{u'v'}}{a\cos\phi}\frac{\partial \bar{v}}{\partial\lambda} - \overline{v'v'}\frac{\partial \bar{v}}{a\partial\phi} + \overline{u'u'}\bar{v}\frac{\tan\phi}{a} \}\, w\, dm \qquad (12)$$

$$C_m = \overline{Z' \{ \bar{\omega}(p_s) - \bar{\mathbf{V}}(p_s) \cdot \nabla p_s \}}^{s} \qquad (13)$$

$$S_a = \int \gamma \overline{T'Q'}\, w\, dm \qquad (14)$$

$$S_k = \int \overline{\mathbf{V}'\mathbf{F}'}\, w\, dm \qquad (15)$$

$$F_e = -\int \nabla \cdot w\, \overline{\phi'\mathbf{V}'}\, dm \qquad (16)$$

$$F_a = -\int \nabla \cdot 1/2\, c_p \gamma w \overline{T'^2\mathbf{V}'}\, dm \qquad (17)$$

$$F_k = -\int \nabla \cdot 1/2\, w \overline{\mathbf{V}'^2\mathbf{V}'}\, dm \qquad (18)$$

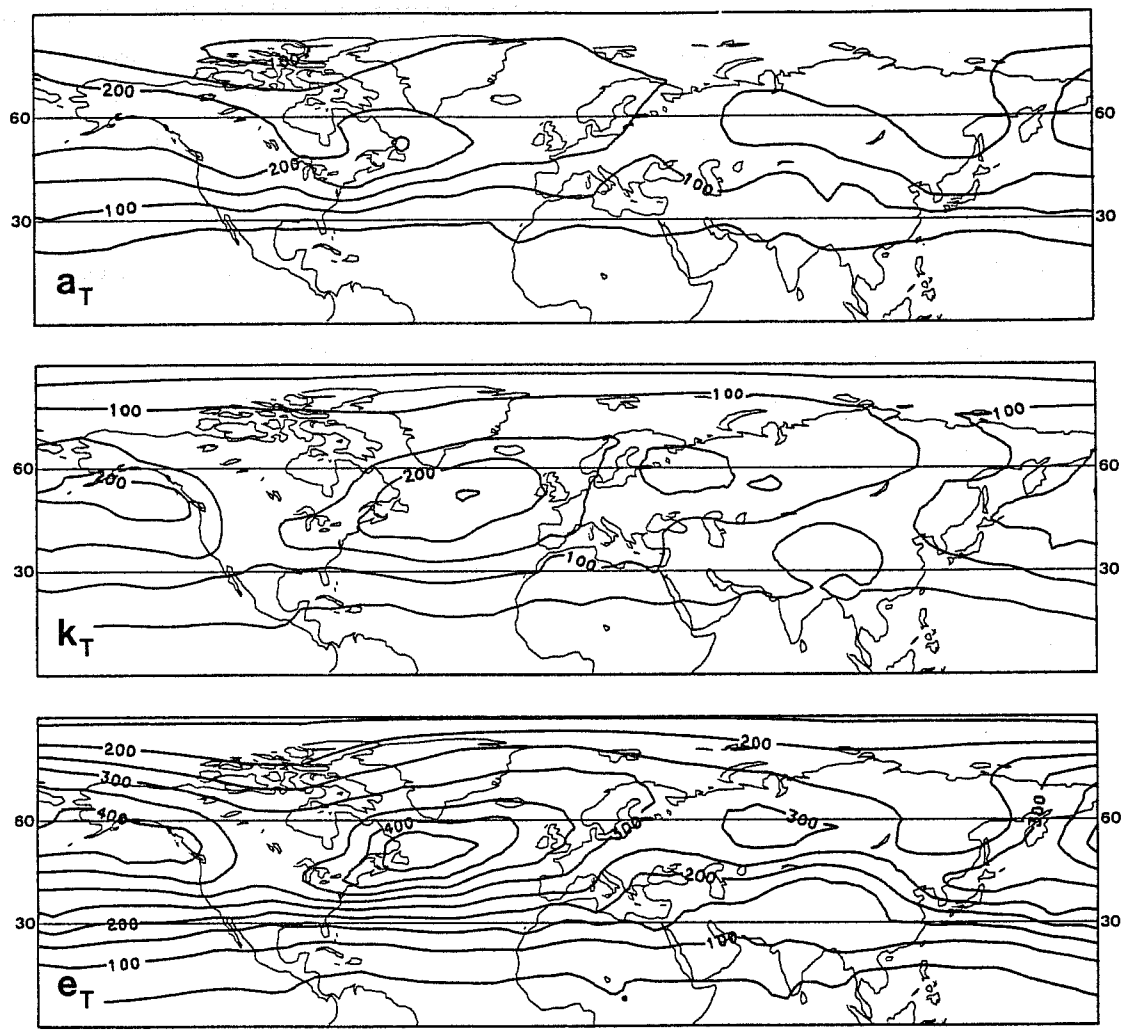

Fig. 10 Distribution of $a_T = 1/2\ c_p\ \gamma\ \overline{T'^2}$ *(upper panel),* $k_T = 1/2\ \overline{\mathbf{V}'^2}$ *(middle panel) and* $e_T = a_T + k_T$ *(lower panel) in December-February at 500 mb, as determined from the GFDL data. Unit:* $J\ kg^{-1}$.

In these expressions $\int ( )\, dm = \int_0^{P_{max}} ( )\frac{dp}{g}$, where P_{max} is the maximum value of surface pressure P_s during the time period considered. The weighting factor $w = w(\lambda,\phi,p)$ measures the fraction of the total sampling time for which the pressure p existed in that geographical location; in a point in the free atmosphere where pressure is always smaller than the minimum surface pressure during the period considered, $w = 1$ (Holopainen, 1970). The operator $\overline{(\ )}^s$ in (13) denotes time-average at the surface. In the expressions for C_a and C_k the contributions of the TE vertical fluxes have been neglected. Furthermore, steady-state condition has been assumed in (9).

The term Adv is the local tendency for e_T change due to horizontal mean-flow flux divergence. The C, S and F terms refer respectively to conversion (from the time-mean flow), source/sink and flux convergence of the TE energy. The terms C_a and C_k and C_m could be called, respectively, the "baroclinic", "barotropic" and "mountain-induced" conversion mechanism. The term S_a stands for diabatic source/sink of TE energy and S_k for the effect of sub-grid scale turbulent friction ("dissipation"). The term F_e, formally the convergence of potential energy in transient eddies, physically represents the work done by the environment on the volume considered. F_a and F_k represent, respectively, the flux convergence of a_T and k_T associated with the transient motions, and are third-order quantities in terms of TE variables. The content of energy equation (9) is schematically illustrated in Fig. 11.

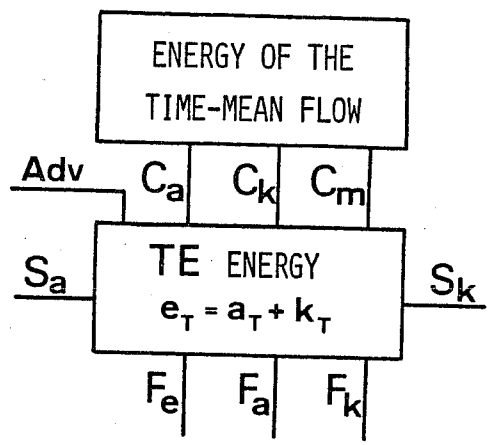

Fig. 11 Local energy diagram for the TE energetics showing the content of Eq. (9) schematically. For the expressions of the terms, see (10) - (18).

The amount of TE energy is thus affected by a number of factors. All of these cannot be estimated from observations. Nevertheless, it is worthwhile to consider, even if qualitatively, the TE energy budget, because the geographical distribution of some budget terms can be estimated reliably from data. This permits a better physical understanding of what is happening than what is often the case with the hemispherically or globally averaged budgets. For example, e_T has at 500 mb (Fig. 10c) such a distribution that if one travels with the time-mean flow eastward from North America at about 50°N, one first experiences an increase of e_T and then, over the Eastern Atlantic, a considerable decrease of e_T. In other words, Adv is negative (positive) west (east) of the maximum of the TE energy. What are the physical processes that bring about this longitudinal varation of e_T?

Conversions C_a and C_k:

The term on the r.h.s. of (9) which can be best estimated from the available data is C_a, for which the pattern in the northern hemisphere winter is shown in the upper part of Fig. 12. This "baroclinic mechanism" produces e_T practically everywhere but particularly so in the cyclogenetic regions near the eastern coasts of the two continents. Note that the American maximum of C_a is considerably stronger than the Asian one. The distribution of C_a has obviously much bearing on the longitudinal distribution of e_T (see Fig. 10 c) and could possibly be useful in the verification of a GCM's ability to simulate the observed TE activity.

The pattern of the "barotropic mechanism" C_k (lower part of Fig. 12) shows large longitudinal variation. Over the oceans at about 30 - 40 °N Fig. 12 shows conversion of mean-flow energy to e_T. Over the northern parts of the oceans, on the other hand, transient eddies feed their energy via C_k to the time-mean flow. This latter feature is compatible with the finding by Holopainen and Oort (1981b), who showed that the transient eddies tend to force cyclonic vorticity in the area of the North Pasific Low and the North Atlantic Low.

A comparison of C_k in Fig. 12 with the calculations reported by Lau (1979a, Fig. 13) for 300 mb shows a fair amount of agreement in some areas but disagreement e.g. over the Atlantic sector. One reason for the differences must be the sensitiviness of the C_k estimates to uncertainties in the basic data. It can be seen from the expression (12) that if the time-mean wind were nondivergent ($\nabla\cdot\bar{\mathbf{V}} = 0$) and the large-scale turbulence isotropic ($\overline{u'u'} = \overline{v'v'}$; $\overline{u'v'} = 0$), C_k would be zero everywhere. Therefore, estimates of C_k depend crucially on statistics like $(\overline{u'u'} - \overline{v'v'})$ and $\overline{u'v'}$, estimates of which are known to

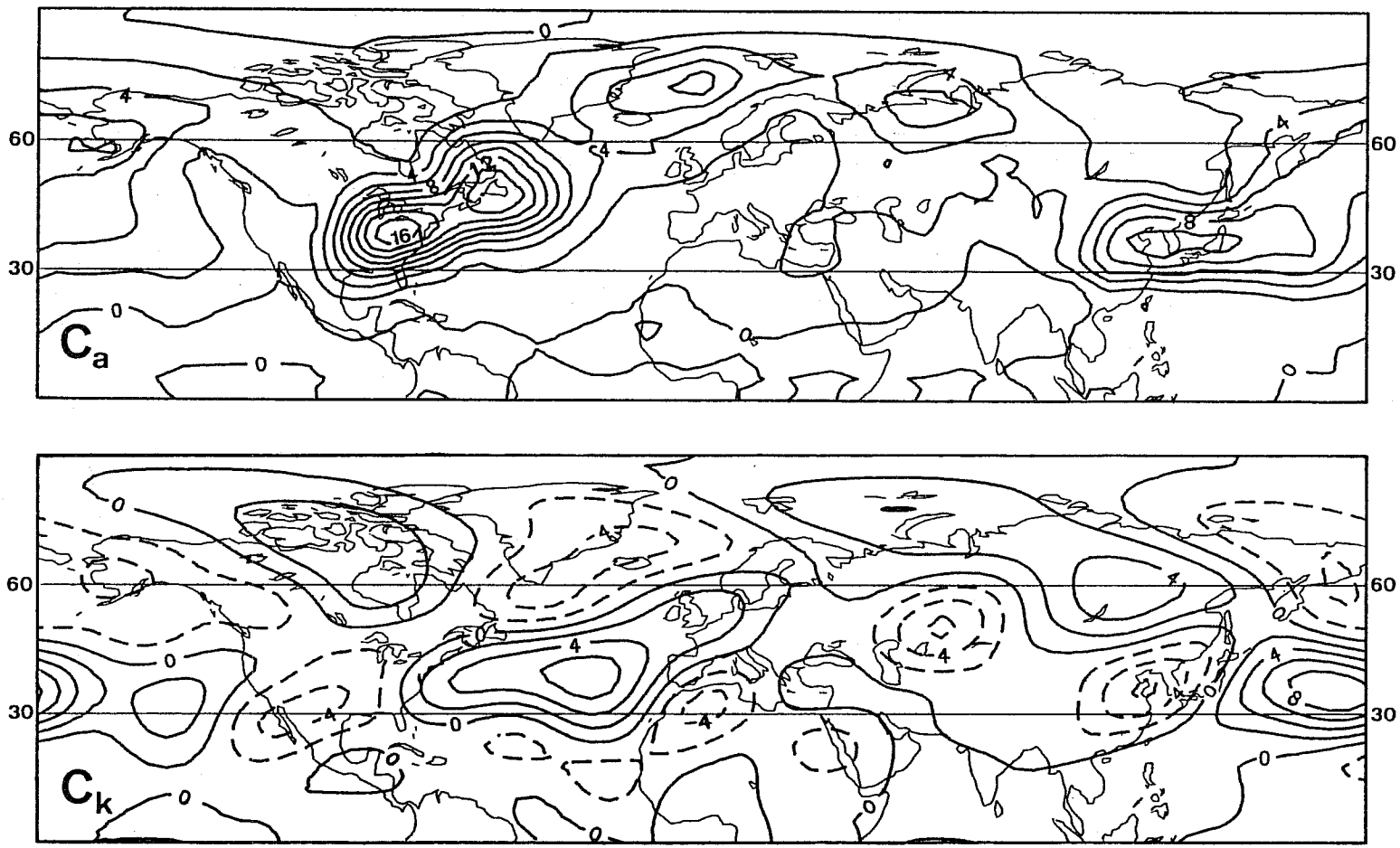

Fig. 12 Distribution of C_a (upper panel) and C_k (lower panel) in December-February, as determined from the 7 FDL data for the 50-1000 mb layer. Unit: W m^{-2}. Isoline spacing is 2 W m^{-2}. (For definitions, see expressions (11) and (12)).

have large margin of uncertainty.

The sum of C_a and C_k (not shown) is positive in most of the extratropics which means that the transient eddies extract energy from the time-mean flow. This result is consistent with the findings of chapter 3.2. concerning the dissipiative effect of TE on the time-mean flow.

Mountain effect C_m:

The expression (13) for the boundary-induced conversion C_m is very difficult to estimate from data (note that $\overline{\omega}$ and $\overline{\mathbf{V}}$, which are time-means in constant pressure, are functions of time in this expression due to the variation of surface pressure). Some idea about the magnitude of this term may be obtained by considering the method in which the effect of mountains is incorporated in the theoretical models of the transient waves. If as the lower boundary is taken an isobaric surface in the lower troposphere, the energetics of the disturbances in the model atmosphere is affected by the mountains through a forced energy flux across this lower boundary. With our notation this flux, which essentially measures the mountain-forced conversion of the mean-flow energy to the TE energy, is given by

$$C_m = - g^{-1} \overline{\Phi' \omega_m'} \quad , \qquad (19)$$

where $\omega_m = - \rho_o g \mathbf{V} \cdot \nabla h$ is the vertical velocity forced by the mountains when ρ_o is (constant) air density and $h = h(\lambda, \phi)$ the surface elevation. By inserting this expression in (19) one obtains

$$\tilde{C}_m = -\rho_o \widetilde{h \nabla \cdot \overline{\Phi' \mathbf{V}'}} \qquad (20)$$

where $\tilde{(\ )}$ denotes an area average over the whole mountain complex. Thus, if mountain areas are associated with a convergence of TE horizontal flux of geopotential, there is a mountain-induced conversion of mean-flow energy into TE energy.

Inspection of the maps (not shown) for $\nabla \cdot \overline{\Phi' \mathbf{V}'}$ as obtained from the GFDL data for the North American region where the data are best shows that at 700 mb in the Rocky Mountains area the amplitude of this term is of the order 5×10^{-4} m^2 s^{-3}, and that its sign varies from place to place. Hence, if we assign 10^3m for h, we get 0.5 W m^{-2} for the magnitude of the local values of $\rho_o h \nabla \cdot \overline{\Phi' \mathbf{V}'}$. However, the magnitude of C_m for the whole area of the Rockies would be considerably smaller because the sign of local contributions varies. We may thus tentatively conclude that the direct mountain-induced

conversion between the mean-flow energy and the transient eddies is rather small even in the mountainous areas (and negligible in hemispheric averages) compared with the "baroclinic conversion" C_a.

However, even if the direct forcing effect of mountains, C_m, on the TE energetics is small, the mountains can still have an important indirect effect by, for example, affecting the baroclinic conversion C_a. Theoretical evidence for this kind of effect has been provided by Sasamori and Youngblut (1981), who show that the baroclinic instability of the planetary waves is enhanced by the presence of forced waves.

Source/sink terms S_k and S_a:

The major part of S_k presumably arises from the atmospheric boundary layer, where it is definitely negative with a hemispheric average of 2-4 W m^{-2} (e.g. Savijärvi, 1981). This boundary layer dissipation is probably largest over the oceanic areas, where k_T has its maximum (Holopainen, 1978). Thus S_k definitely plays an important role in the eastward decrease of TE energy in the Eastern Atlantic (Fig. 10).

There is little empirical information concerning S_a. This term depends on the covariance of the local fluctuation of temperature T and the net diabatic heating Q, which consists of the combined effect of radiation, Q_R, condensation heating Q_C and the heating Q_T due to turbulent exchange: $Q = Q_R + Q_C + Q_T$.

A considerable longitudinal variation is likely to exist in S_a and in the contributions to it from the different heating mechanisms. For example, in the cyclogenetic regions near the eastern coasts of the continents one can expect the condensation heating to make a positive contribution to S_a (i.e. $\overline{T'Q'_C} > 0$), and $\overline{T'Q'_R}$ to be rather small because of the small time-scale of the transient fluctuations in these regions (Blackmon, 1976). Over oceans, however, where long-period transients dominate, S_a is likely to have a damping effect on TE for two reasons. First, radiative effects in the middle and upper troposphere definitely cause cooling e.g. in the warm, cloudless blocking highs which are an important ingredient in the low-frequency variability in the eastern oceans in middle and high latitudes. Secondly, the contact with the warm ocean is likely to damp the cold anomalies, particularly over the western coasts of the oceans, and thus lead to $\overline{T'Q'_T} < 0$ in the lower troposphere.

A pilot estimation of S_a was made by using daily aerological data from six British aerological stations for a 3-month period September - November 1954. The net diabatic heating Q was estimated as the residual term in the thermodynamic energy equation, in which the terms representing local change, horizontal advection and vertical advection of heat were evaluated with the aid of the data. (The vertical velocity ω was calculated from the horizontal divergence by using the continuity equation and the constraint that $\omega = 0$ at 1000 mb and 200 mb). In the middle troposphere (700-300 mb), where the results for the British Isles area are possibly representative for the Eastern Atlantic in general, the calculations resulted in $\gamma\overline{T'Q'} = -2 \times 10^{-5}$ J kg^{-1} s^{-1}. If this value is considered representative for the whole atmospheric column, it implies $S_a = -2$ W m^{-2}. This kind of thermal dissipation is almost comparable to the mechanical dissipation in the boundary layer!

Certain mountain areas may have an important indirect effect on the TE energetics via their effect on S_a. In the cases of warm, moist air flowing over the mountains the orographically induced precipitation can be large and one has a positive contribuiton to $\overline{T'Q'_c}$. Particularly over the Northwestern Rockies and Alaska, where the mountains are on the coast of a relatively warm ocean, this process could in winter make S_a positive and possibly be a reason for the particularly large values of a_T in the low troposphere in these regions, as evident from Fig. 1a.

Flux convergence terms F_e, F_a and F_k:

From the flux convergence terms the physically most important one is the "energy dispersion" term F_e (which would also be present in small-amplitude wave models in which the third-order terms F_a and F_k are negligible). Fig. 13 shows the map of $\nabla \cdot \overline{\Phi' V'}$ for 300 mb in winter according to Lau and Wallace (1979). Flux divergence (convergence) is indicaded e.g. on the northwestern (southwestern) side of the typical cyclone tracks at the eastern coast of North America. These features are also obtained from the GFDL data, from which one gets 5-10 W m^{-2} for the magnitude of F_e over eastern North America. Energy dispersion can thus play a significant role in local energy budgets. As known from several observational studies (e.g. Oort and Rasmusson, 1971) the wintertime extratropics north of 30°N experiences an average loss in TE energy of about 0.5 W m^{-2} due to this dispersion.

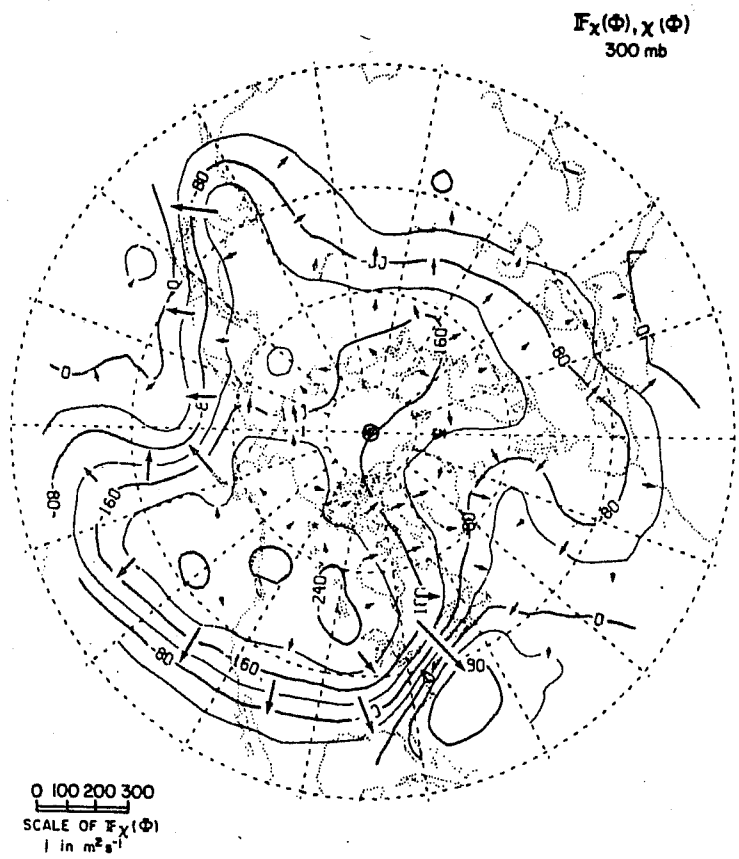

Fig. 13 Contours show the velocity potential χ for the irrotational TE flux of geopotential height ($\nabla^2\chi = \nabla\cdot\overline{Z'\mathbf{V}'}$) at 300 mb, the vectors the irrotational flux ($\overline{Z'\mathbf{V}'}_\chi$ itself. (From Lau and Wallace, 1979, Fig. 2)

Stable values of the third-order terms F_a and F_k require large data samples. Lau (1979) has reported calculations of F_k for 300 mb using NMC data. Inspection of his Fig. 13 reveals that in western Europe and western North America, which are downstream from the oceanic maxima of k_T, F_k is positive and important in the local budget of k_T. Our unpublished calculations using European aerological data indicates that F_a is positive in winter over western Europe and important in the local budget of a_T.

Summary of TE energetics:

The semi-quantitative considerations presented above indicate that none of the terms in the TE energy equation (9) is generally negligible. Fig. 14 shows an energy diagram for an atmospheric column over eastern North America and the Eastern Atlantic at about 50^{o}. It also answers the question raised earlier concerning the reasons for the Atlantic maximum of a_T. As one might have expected on the basis of synoptic experience and earlier studies, the "baroclinic mechanism" C_a appears to be primarily responsible for this feature. The rapid eastward decrease of e_T over the Eastern Atlantic is probably not only due to frictional dissipation but also due to thermal damping of e_T. Energy dispersion also plays an important role in both regions. In the eastern Atlantic the third-order terms are probably also significant.

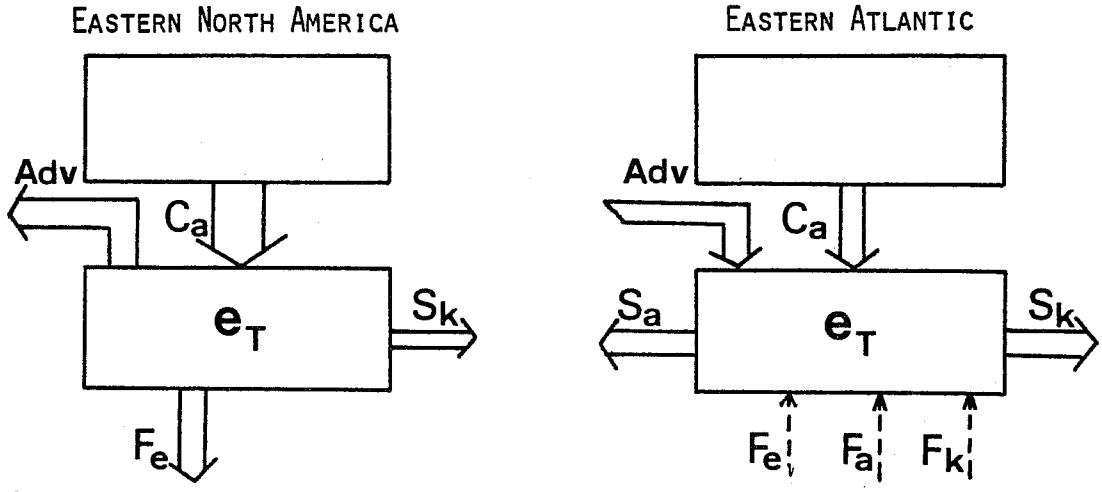

Fig. 14 Dominant terms in the local TE energy diagram (described schematically in Fig. 11) for "Eastern North America" and "Eastern Atlantic". The thickness of the arrows is proportional to the relative importance of the process in question. The dashed arrows indicate processes, estimates of which are either uncertain or sensitive to the exact location of the air column. Rough numerical values for some of these processes are given in the text.

Most of the uncertainties in the above analysis (like those associated with F_e, F_a and F_k) can in principle be removed with improved data and data analysis schemes. Questions concerning the diabatic heating effects are, however, intrinsically more difficult and require special effort. A proper simulation of S_a with the GCM's requires that not only the surface fluxes, convection and condensation processes but also clouds and their influence on radiation be properly treated in the model.

4. WHAT COULD BE DONE IN THE AREA OF DIAGNOSTIC ANALYSIS OF "OBSERVED" AND "CALCULATED" CLIMATE

The discussion presented in chapters 2 and 3 suggests some areas in which research should be done in future:

Confidence limits for the "observed" climate:

A comprehensive intercomparison of grid-point analyses made in different centers from essentially the same input data should be made for example along the lines followed by Arpe (1980) in order to further improve our knowledge concerning the uncertainties in the "observed" conditions. One useful data set for this purpose is that gathered in connection with the WMO/CAS NWP project (Bengtsson and Lange, 1981). Special importance must be given to the comparison of the different global (level III) FGGE data. A comparative study should be made of the two level IIIb data sets produced by ECMWF and GFDL; this intercomparison would probably gain further significance if some operational (level IIIa) FGGE data sets were included in it.

Verification of a GCM:

In comparison of the long-period statistics from a GCM with the corresponding "observed" quantities one should pay attention to the geographical distribution not only of the time-mean fields but also to some second-order statistics such as variances. An example of model verification of this kind is that reported by Blacmon and Lau (1981). It indicates that the particular model studied has a relatively realistic time-mean flow but does not simulate the observed low-frequency variability of the atmosphere very well. In addition to variances other useful quantities, which could be used to look at the model's ability to produce the right TE activity, are the "observed" and "calculated" fields of the eddy forcing parameter χ_q and the baroclinic conversion mechanism C_a discussed in sections 3.2 and 3.3, respectively.

In the verification of advanced GCM's it is also probably time to begin, in addition to the verfication of the large-scale circulation, a special verification in some continental regions in which good information exists e.g. for such important climate variables as precipitation and run-off, and in which good model performance is of particular importance.

Diabatic processes:

Interesting results have been recently reported e.g. by Schubert and Herman (1981), Wei et al.(1982) and Savijärvi (1981) on diabatic heating in the atmosphere. It is likely that with the improved analysis techniques the "residual method" can provide estimates of the geographical distribution of the net diabatic heating not only for the time-mean conditions but also for the long-period transients. If the individual heating components Q_R, Q_C and Q_T are estimated simultaneously by using the modern parametrization schemes, significant new information can possibly be obtained on the role of diabatic processes in the maintenance of the different modes of atmospheric circulation. A potentially useful parallel approach for the study of these processes should be detailed case studies, such as that reported by Tiedke (1979).

ACKNOWLEDGEMENTS

I am very much indebted to Drs. A.H. Oort and N-C. Lau, Geophysical Fluid Dynamics Laboratory (Princeton, USA) for allowing part of their data sets ("GGDL data" and "NMC data", respectively) to be used in some of the analyses reported here, and for collaboration on several papers referred to in this contribution. Technical assistence has been provided by L. Rontu and P. Nurmi in the Department of Meteorology, University of Helsinki.

REFERENCES

Arpe, K., 1980: Confidence limits for the verification and energetics studies. Tech. Report No. 18, ECMWF.

Atlas, D. and O. W. Thiele, 1982: Precipitation measurements from space: workshop summary 29 April - 1 May, 1981. Greenbelt, Md. Bull. Amer. Met. Soc., 63, 59-63.

Bengtsson L. and A. Lange, 1982: Results of the WMO/CAS Numerical Weather Prediction Data Study and Intercomparison Project for forecasts for the Northern Hemisphere in 1979-80. World Meteorological Organization, Geneve.

Bengtsson L., M. Kanamitsu, P. Kållberg and S. Uppala, 1981: Diagnostic and predictability studies using FGGE data. Seminars on problems and prospects in long and medium range weather forecasts, (ECMWF, Reading), pp. 405-428.

Berlyand, T.G. and L.A. Strokina, 1980: Global distribution of a cumulative number of clouds (in Russian). Hydrometor. Publish. House, Leningrad.

Blackmen, M.L., 1976: A climatological spectral study of the 500 mb geopotential height of the Northern Hemisphere. J. Atmos. Sci., 33, 1607-1623.

Blackmon, M.L. and N-C. Lau, 1980: Regional characteristics of the Northern Hemisphere wintertime circulation: A comparison of the simulation of a GFDL general circulation model with observations. J. Atmos. Sci.,37, 497-514.

Budyko, M.I. (Ed.), 1963: Atlas of the heat balance of the world. (In Russian). Kartafabrika Goegeoltehizdata, Leningrad.

Edmon, H.J., B.J. Hoskins and M.E. McIntyre, 1980: Eliassen-Palm cross sections for the troposphere. J. Atmos. Sci., 37, 2600-2616.

Hastenrath, S., 1980: Heat budget of tropical ocean and atmosphere. J. Phys. Oceanography, 10, 159-170.

Holopainen, E.O., 1970: An observational study of the energy balance of the stationary disturbances in the atmosphere. Quart. J. Roy. Met. Soc., 96, 626-644.

Holopainen, E.O., 1978: A diagnostic study of the kinetic energy balance of the long-term mean flow and the associated transient fluctuations in the atmosphere. Geophysica, 15, No. 1, 125-145.

Holopainen, E.O., L. Rontu and N-C. Lau, 1982: On the effect of large-scale transient eddies on the time-mean flow in the atmosphere. J. Atmos. Sci., xxx-xxx.

Holopainen, E.O. and A.H. Oort, 1981a: Mean surface stress curl over the oceans as determined from the vorticity budget of the atmosphere. J. Atmos. Sci., 38, 262-269.

- " -, 1981b: On the role or large-scale transient eddies in the maintenance of the vorticity and enstrophy of the time-mean atmosphere flow. J. Atmos. Sci., 38, 270-280.

Jaeger, L., 1976: Monatskarten der Niederschlage für die ganze Erde. Ber. Dtsch. Wetterd., 18, No. 139.

JOC, 1979: Report of the JOC Study Conference on climate models: performance, intercomparison and sensitivity studies. GARP Publication Series No. 22. WMO Secretariat, Geneve.

Lau, N-C., 1979a: The structure and energetics of transient disturbances in the Northern Hemisphere wintertime circulation. J. Atmos. Sci., 36, 982-995.

Lau, N-C, 1979b: The observed structure of the tropospheric stationary waves and the local balances of vorticity and heat. J. Atmos. Sci., 36, 996-1016.

Lau, N-C, and J. M. Wallace, 1979: On the distribution of horizontal transports by transient eddies in the northern wintertime circulation.J. Atmos. Sci., 36, 1844-1861.

Lau, N-C and A.H. Oort, 1981: A comparative study of observed Northern Hemisphere circulation statistics based on GFDL and NMC analyses. Part I: The time-mean fields. Mon. Wea. Rev., 109, 1380-1403.

Lau, N-C, and A. H. Oort, 1982: A comparative study of observed Northern Hemisphere circulation statistics based on GFDL and NMC analyses. Part II: Transient eddy statistics and the energy cycle. Mon. Wea. Rev., 110,...

Lau, N-C, G.H. White and R.L. Jenne, 1981: Circulation statistics for the extra-tropical Northern Hemisphere based on NMC analyses. NCAR Tech. Note TN-171+ STR, 138 pp.
Available from: Publication Office of NCAR, National Center for Atmospheric Research, Boulder. Co 80307, USA.

van Loon, H., 1979: The associaton between latitudinal temperature gradient and eddy transport. Part I: Transport of sensible heat in winter. Mon. Wea. Rev., 107, 525-534.

Madden, R.A., 1976: Estimates of the natural variability of time-averaged sea-level pressure. Mon. Wea. Rev., 104, 942-952.

Newell, R.E., J.W. Kidson, D.G. Wincent, G.J. Beer, 1972/1974: The general circulation of the tropical atmosphere and interactions with extratropical latitudes. Vol. I/II. The MIT Press, 258/371 pp.

Oort, A.H. 1964: On estimates of atmospheric energy cycle. Mon. Wea. Rev., 92, 483-493.

Oort, A.H. and J.P. Peixoto, 1976: On the variability of the atmospheric energy cycle within a 5-year period. J. Geop. Res., 81, 3643-3659.

Oort, A.H., 1977: The interannual variability of atmospheric circulation statistics, NOAA Professional Paper 8, 1-76.

Oort, A.H., 1978: Adequacy of the radiosonde network for global circulation studies tested through numerical model output. J. Atmos. Sci., 106, 174-195.

Oort, A.H., 1982: Global atmospheric circulation statistics, 1958-1973. NOAA Professional Paper (in preparation).

Oort, A.H., and E.M. Rasmusson, 1971: Atmospheric Circulation Statistics. NOAA Prof. Paper 5, U.S. Government Printing Office, Washington DC NTIS COM-72-50295.

Parker, D.E., 1980: Climate change or analysts' artifice? - a study of grid-point upper air data. The Meteor. Mag., 109, 129-152.

Peixoto, J.P. and A.H. Oort, 1974: The annual distribution of atmospheric energy on a planetary scale. J. Geoph. Res., 79, 2149-2159.

Sasamori, T. and C.E. Youngblut, 1981: The nonlinear effects of transient and stationary eddies on the winter mean circulation. Part II: The stability of stationary waves. J. Atmos. Sci., 18, 87-96.

Savijärvi, H., 1981: The energy budgets in North America, North Atlantic and Europe based on ECMWF analyses and forecasts. ECMWF Tech. Rep. No 27.

Schiffer, R.A., 1982: The international Satellite Cloud Climatology Project (ISCCP): Preliminary Implementation Plan. Available from the WCRP Office, WMO Secretariat, Geneve.

Schubert, S.D., and G.F. Herman, 1981: Heat balance statistics arrived from four-dimensional assimilations with a global circulation model. J. Atmos. Sci., 38, 1891-1905.

Speth P. and G. Frenzen, 1982: Variability in time of horizontal transports of heat and momentum by stationary eddies. Beitr. Phys. Atmosph., 55, 142-157.

Stephens, G.L., G.C. Campbell and T.H. Vonder Haar, 1981: Earth radiation budgets. J. Geoph. Res., 86, No. C10, 9739-9760.

Tiedke, M., 1977: Numerical tests of parametrization schemes at an actual case of transformation of arctic air. ECMWF Internal Report No. 10.

Trenberth, K.E., 1981: Interannual variability of the Southern Hemisphere 500 mb flow: regional characteristics. Mon. Wea. Rev., 109, 127-136.

Trenberth, K.E. and Daniel A. Paolino, Jr., 1980: The Northern Hemisphere sea-level data set: trends, errors and discontinuities. Mon. Wea. Rev., 108, 855-872.

White, G.H., 1982: An observational study of the Northern Hemisphere extratropical summertime general circulation. J. Atmos. Sci., 39, 24-40.

UNESCO, 1974: World Water Balance and Water Resources of the Earth. Studies and and reports in Hydrology No. 25. Prepared by the USSR Nat. IHD Comm. English translations 1977, 1978.

Wei, M-Y, D.R. Johnson and R.D. Townsend, 1982: Seasonal distribution of diabetic heating during the first GARP global experiment. Tellus, 34, xxx-xxx.

Youngblut, C. and T. Sasamori, 1980: The nonlinear effects of transient and stationary eddies on the winter mean circulation. Part I: Diagnostic analysis. J. Atmos. Sci., 37, 1944-1957.